

# Preparation of Starch Nanoparticles in a New Ionic Liquid-in-Oil Micro-emulsion

Luo Zhigang<sup>1\*</sup>, She Linrong<sup>2</sup> and Zhan Meina<sup>2</sup>

<sup>1</sup>Carbohydrate Lab, School of Food Science and Engineering, South China University of Technology, Guangzhou, China

<sup>2</sup>Heng Sheng Wei Jia Food Industry Co., Ltd, Chaozhou, China

## Abstract

In this work, a new room-temperature ionic liquid 1-hydroxypropyl-3-methylimidazolium acetate ([C<sub>3</sub>OHmim]Ac) was synthesized to dissolve starch and substitute for polar phase to form [C<sub>3</sub>OHmim]Ac/TX-100+1-butanol/cyclohexane micro-emulsions. The molecular structure of [C<sub>3</sub>OHmim]Ac was confirmed by means of <sup>1</sup>H nuclear magnetic resonance (<sup>1</sup>HNMR) and electrospray ionization mass spectrometry (ESI-MS). Pseudo-ternary phase diagram, conductivity measurement and dynamic light scattering (DLS) were used to analyze the microregion of IL/O micro-emulsion. Starch nanoparticles were prepared in this novel IL/O micro-emulsion with octenyl succinic anhydride (OSA) maize starch as the raw material and epichlorohydrin as the cross-linker. Fourier transform infrared spectroscopy (FTIR) data demonstrated the formation of crosslinking bonds in starch molecules. The spectrum of XRD suggested that the crystal structure of starch was destroyed. Scanning electron microscopy (SEM) and dynamic light scattering (DLS) both intuitively revealed that starch nanoparticles had good sphericity, small size and a relatively concentrated size distribution with the mean diameter of starch nanoparticles 105 nm.

**Keywords:** Ionic liquid; Ionic liquid micro-emulsion; Cross-linking; Starch nanoparticle

## Introduction

As one of the most abundant natural materials, starches have their own merits like renewable, biodegradable, cost-effective. However, when applied to food and pharmaceutical fields, native starches usually need to be modified through physical, chemical, or enzymatic methods to overcome some limitations such as low thermal resistance, poor processability and solubility [1-4]. Among these starch derivatives, cross-linked starch microspheres, have attracted great interests due to their high resistance towards swelling, high shear, compression and acidic conditions and also have been one of the most investigated drug carriers for their biodegradability, biocompatibility, non-toxicity as well as high surface area [4-10].

In the last decade, papers have reported the preparation of cross-linked starch microspheres relying on solvent evaporation, precipitation and spray drying or emulsion-crosslinking techniques. Among these methods, water-in-oil (W/O) micro-emulsion has been thought as the economic and convenient template for preparing starch microsphere. There into Mao et al. reported the preparation of starch microspheres with the mean diameter ranging from 30 to 60 μm [11-14]. Mao et al. estimated the average diameter of the micro-particles synthesized by W/O emulsification-cross linking method to be 50 μm [14]. However, excessively large size and broad size distribution of starch microspheres have always been the problems in the traditional W/O emulsion cross-linking technique, which not only increase the risk of merging or rupturing of microspheres in tableting, but also limit the uniform and sustained release in drug delivery. In this context, there is a strong incentive to develop a new strategy for the synthesis of starch nano-sized particles with a narrow size-distributed region and research their drug delivery properties [10-12].

In recent years, room-temperature ionic liquids (ILs) have been considered as possible green and effective replacements for polar phase, non-polar phase or surfactant to prepare ionic liquid micro-emulsions, and synthesis of various inorganic particles in IL micro-emulsions system have been studied. Nevertheless, due to the structural complexity and diversity, the meticulous study on formation

of starch microspheres using ILs micro-emulsion system have rarely been explored, much less for nanoparticles. In the previous reports by our group, much progresses in applying ILs into starch chemistry have been acquired in terms of dissolution and esterification of starch. These works show that ILs containing Cl<sup>-</sup>, Ac<sup>-</sup> and NO<sub>3</sub><sup>-</sup> anions, like 1-butyl-3-methylimidazolium chloride ([Bmim]Cl), 1-ethyl-3-methylimidazolium acetate ([Emim]Ac) and 1-octyl-3-methylimidazolium acetate ([Omim]Ac), can dissolve starch by destroying the crystalline structure and disrupting hydrogen bonding among hydroxyl groups of polymers effectively. Thereby, it enlightened us that the resulting stable and uniform dispersion of starch molecules in suitable ILs is capable of creating the excellent environment for the formation of starch nanoparticles. Accordingly, ILs with good dissolubility to starch is a prerequisite for establishing the starch nanoparticles [14].

In this work, a new room-temperature ionic liquid 1-hydroxypropyl-3-methylimidazolium acetate ([C<sub>3</sub>OHmim]Ac) based on the hydroxy-functionalized imidazolium cation was tailor-made, which was the first reported by us to dissolve starch, and its molecular structure was systematically confirmed by means of <sup>1</sup>H nuclear magnetic resonance (<sup>1</sup>HNMR) and electrospray ionization mass spectrometry (ESI-MS). Then the new IL acted as the polar phase, combining surfactant polyethylene glycol octylphenol ether (TX-100), cosurfactant 1-butanol and oil phase cyclohexane, to prepare [C<sub>3</sub>OHmim]Ac/TX-100+1-butanol/cyclohexane nonaqueous ionic liquid micro-emulsions. Different techniques were used to characterize the microstructure of micro-emulsions, including pseudo-ternary phase diagram,

**\*Corresponding author:** Luo Zhigang, Professor, School of Food Science and Engineering, South China University of Technology, Guangzhou, China. Tel: +86-20-87113845; E-mail: zhgluo@scut.edu.cn

Received October 25, 2017; Accepted November 05, 2017; Published November 15, 2017

**Citation:** Zhigang L, Linrong S, Meina Z (2017) Preparation of Starch Nanoparticles in a New Ionic Liquid-in-Oil Micro-emulsion. J Formul Sci Bioavailab 1: 116.

**Copyright:** © 2017 Zhigang L, et al. This is an open-access article distributed under the terms of the Creative Commons Attribution License, which permits unrestricted use, distribution, and reproduction in any medium, provided the original author and source are credited.

conductivity measurement and dynamic light scattering (DLS). Starch nanoparticles were prepared in this novel IL/O micro-emulsion with OSA maize starch as the raw material, epichlorohydrin as the cross-linker and characterized by Fourier transform infrared spectroscopy (FTIR), X-ray diffraction (XRD), scanning electron microscopy (SEM) and DLS. Finally, drug loading and releasing properties of starch nanoparticles were investigated with indomethacin as a drug model [15,16].

## Material and Methods

### Materials

1-Methylimidazole, 1-Chloro-3-hydroxypropane was purchased from Aladdin Chemical Reagent Company (Shanghai, China). Native maize starch was obtained from ChangChun DaCheng Maize Products Co. (Changchun, China). TX-100 was obtained from Sinoparm Chemical Reagent Co., Ltd (Shanghai, China). OSA was purchased from Gutian Chemical Engineering Co., Ltd (Nanjing, China). All other chemicals were of analytical grade [17].

### Synthesis of ionic liquid [C<sub>3</sub>OHmim]Ac

[C<sub>3</sub>OHmim]Ac was prepared in two steps (Figure 1). 1-methylimidazole (0.5 mol) and 1-Chloro-3-hydroxypropane (0.6 mol) were added in three-neck round flask with a reflux condenser for 12 h at 70°C with stirring under nitrogen. The reaction solution was cooled to room temperature and washed with ethyl acetate for three times. The bottom phase was collected, heated at 70°C for 12 h to get intermediate 1-hydroxypropyl-3-methylimidazolium chloride ([C<sub>3</sub>OHmim]Cl). After that, potassium acetate (0.34 mol) and [C<sub>3</sub>OHmim]Cl(0.28 mol) were dissolved in right amount of methanol, the mixture was stirred at 25°C for 24 h. After reaction, the solid was removed by negative-pressure filtration and methanol was removed under vacuum. The residue was washed with diethyl ether to remove the unreacted potassium acetate under reduced pressure. The product were heated at 50°C for 24 h to get [C<sub>3</sub>OHmim]Ac with 91% of yield.

The structure of ionic liquid [C<sub>3</sub>OHmim]Ac was characterized by <sup>1</sup>HNMR and ESI-MS as follows. The <sup>1</sup>H-NMR spectra were obtained with an Avance III 600 MHz digital NMR spectrometer using DMSO as solvent. The ESI-MS spectrum was obtained under positive ion mode by using Electro-spray mass spectrometry [18].

### Preparation of ionic liquid micro-emulsions

To prepare [C<sub>3</sub>OHmim]Ac/TX-100+1-butanol/cyclohexane ionic liquid micro-emulsions, certain amount of [C<sub>3</sub>OHmim]Ac and cyclohexane weighted by an analytical balance (d=0.0001 g, FA1104N, Shanghai Balance Instrument Co., Shanghai, China) were added in a

small beaker, then the mixture of surfactant TX-100 and cosurfactant 1-butanol with the mass ratio at 1 to 1 was added into the solution until the turbid solution became homogeneous and transparent.

### Pseudo-ternary phase diagram

The phase behavior of [C<sub>3</sub>OHmim]Ac/TX-100+1-butanol/cyclohexane micro-emulsions system was determined at 25°C by direct observation method. Series of the micro-emulsions were prepared by fixing weight ratio of [C<sub>3</sub>OHmim]Ac/cyclohexane at 9:1, 8:2, 7:3, 6:4, 5:5, 4:6, 3:7, 2:8, 1:9, and shaken sharply in a vortex mixer. After thermal equilibrium, the mixture of surfactant TX-100 and co-surfactant 1-butanol was added drop by drop until the phase transition was observed from turbidity to transparency [19-21].

### Conductivity measurement

Conductivity of ionic liquid micro-emulsions were measured by means of a conductometer (DDS-307, Shanghai Precision Scientific Instrument Co., Shanghai, China) at 1 kHz using a dip-type cell of cell constant 0.971 cm<sup>-1</sup>. TX-100 and 1-butanol were mixed by the mass ratio of 1:1, which was used as surfactant. The cyclohexane was progressively added into the mixture of surfactant and [C<sub>3</sub>OHmim]Ac, and the conductivity was measured after shaken in a vortex mixer. The errors in the conductance measurements were ±0.5%.

### Preparation of OSA modified maize starch

Amount of native maize starch (dry weight) was suspended in distilled water (35%, w/w) with agitation at 35°C. The pH of the mixture was adjusted with a pH controller (Model 501-3400, Barnant Co.) at 8.5-9.0 by adding 3% NaOH solution. 3% (based on dry starch dry) of OSA was added slowly within 2 h while controlling the pH at 8.5-9.0. After adding OSA, the reaction continued for another 1 h. After reaction, the mixture was adjusted to pH 6.5 with 3% HCl solution, and then centrifuged and washed twice with distilled water and twice with 95% (v/v) ethanol. The sample was oven-dried at 40°C for 24 h and then passed through a 100-mesh nylon sieve.

Determination of the Degree of Substitution (DS): The DS of OSA starch was measured by titration. OSA starch (5 g, dry starch basis) was accurately weighted and suspended in 25 mL of 2.5 mol/L HCl-isopropyl alcohol solution by stirring 30 min. Then 100 mL of 90% isopropyl alcohol solution (v/v) was added and stirred for a further 10 min. The suspension was filtered through a glass filter, then the residue was washed with 90% isopropyl alcohol solution until no Cl<sup>-</sup> could be detected by using 0.1 mol/L AgNO<sub>3</sub> solution. The starch was re-dispersed in 300 mL of distilled water and heated in a boiling water bath for 20 min. The starch solution was titrated with 0.1 mol/L standard NaOH solution using phenolphthalein as an indicator. A

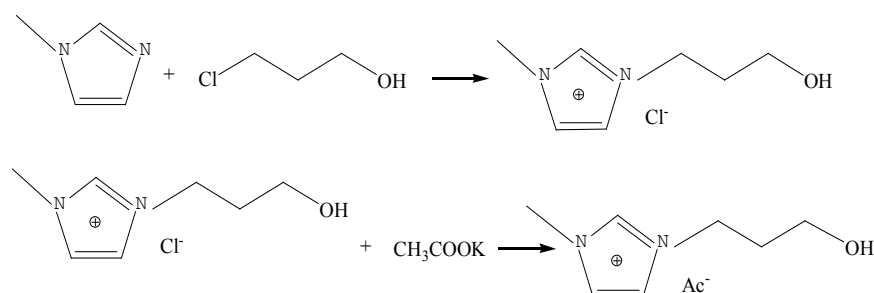


Figure 1: Preparation of ionic liquids [C<sub>3</sub>OHmim]Ac by two-step method.

blank was simultaneously titrated with native corn starch as a sample. The DS was calculated as follow:

$$DS = \frac{0.162 \times (A \times M) / W}{1 - [0.209 \times (A \times M) / W]} \quad (1)$$

where A is the titration volume of NaOH solution (mL), M is the molarity of NaOH solution, W is the dry weight (g) of the OSA starch. According to the calculation, the DS of the modified starch was 0.018 [22].

### Preparation of starch nanoparticles

Starch nanoparticles were produced by [C<sub>3</sub>OHmim]Ac/TX-100+1-butanol/cyclohexane ionic liquid micro-emulsions cross-linking method with OSA starch as the raw material and epichlorohydrin as the cross-linker. Dried OSA starch was dissolved into [C<sub>3</sub>OHmim]Ac at a concentration of 2% (w/w) in a three-neck round flask which was full of gaseous N<sub>2</sub>, the mixture was stirred by mechanical agitation (JB90-B, Shanghai Standard Model Co., Shanghai, China) at 90°C for 3 h to prepare the water phase. Then cyclohexane was added into the water phase with a mass ratio of 7 to 1, 45% (w/w) of the mixture of TX-100 and 1-butanol with the mass ratio of 1:1 was added subsequently to bulid IL/O micro-emulsion. After stirring for several minutes, 2% (w/w) epichlorohydrin was added to the micro-emulsion as a cross-linker agent. In this stage, the reaction was controlled at the condition of 50°C for 3 h. The resulted micro-emulsion was cooled to the room temperature, and then starch nanoparticles were precipitated by anhydrous ethanol and centrifuged. The residue was washed with sufficient anhydrous ethanol to eliminate IL, cyclohexane, TX-100, 1-butanol and unreacted epichlorohydrin. Finally, the product was obtained after dried at 40°C for 24 h. In addition, starch nanoparticles with different particle sizes could be obtained through changing the reaction conditions such as reaction time, reaction temperature, and starch concentration [23-25].

### Characterization of starch nanoparticles

The structural characteristics of native maize starch, OSA starch and starch nanoparticles was evaluated by FTIR spectroscopy. For FTIR measurement, the samples were mixed with dried KBr and then compressed into thin disk-shaped pellets. The wave numbers of FTIR spectra ranged from 400 to 4000 cm<sup>-1</sup> with a resolution of 1 cm<sup>-1</sup>.

X-ray diffraction (XRD) technique was used to analyze the crystal structure of native maize starch, OSA starch and starch nanoparticles. XRD spectra was obtained on a X-ray diffractometer (D/Max2200, Bruke Co., Germany) with Cu Ka radiation (λ=0.154 nm) at 40 kV and 40 mA, the scattering angle rang (2θ) was 0~60° at a scattering speed of 0.02°/min.

The morphology of native maize starch, OSA starch and starch nanoparticles were characterized through Scanning electron microscopy (Merlin scanning electron microscope, Zeiss Co., Germany). All the samples were gold coated before morphology observation.

Laser light diffraction technique was used to evaluate the particle size and particle size distribution of starch nanoparticles. 0.05 g starch nanoparticles were dispersed in 100 mL distilled water and treated by ultrasound for 30 min before measurement to prevent agglomeration [26-28].

### Standard Curves of indomethacin

Standard curves of indomethacin were obtained using the following approaches: 0.05 g of indomethacin was fully dissolved in

25 ml anhydrous ethanol, then diluted to 500 ml with phosphate-buffered saline (PBS, 0.2 mol/L, pH 7.4). The obtained 0.01 mg/mL of indomethacin in PBS solution was scanned at wavelengths between 190 and 550 nm with a model TU-1810 ultraviolet-visible spectrophotometer (Beijing Puxi General Apparatus Co., Ltd., Shanghai, China). The wavelength at which indomethacin absorbed the most was selected as the testing wavelength for later experiments, then 0.01, 0.02, 0.03, 0.04, and 0.05 mg/mL of indomethacin in PBS solution were measured at the corresponding testing wavelengths to obtain the standard curve of indomethacin absorbance to concentration.

### Drug loading analysis

About 50 mg of starch nanoparticles with diameters were weighed and suspended in 20 mL of PBS solution with 0.02, 0.04, 0.06, and 0.08 mg/mL indomethacin each. The resulting suspensions were gently stirred at the desired temperature of 17, 27, 37, and 47°C for 0.5, 1, 1.5, 2 and 2.5 h. Subsequently, the solutions were centrifuged, and each supernatant was extracted to determine the drug loading and encapsulation efficiency with an ultraviolet-visible spectrophotometer according to the standard curve of indomethacin absorbance to concentration. The drug loading (A) and encapsulation efficiency (B) were calculated with eqns. (2) and (3), respectively.

$$A = (C_0 - C_1V_1)V_0 / W \quad (2)$$

$$B = (C_0 - C_1V_1) / C_0 \quad (3)$$

where C<sub>0</sub> means initial concentration of indomethacin in PBS solution, C<sub>1</sub> means diluted concentration of indomethacin in PBS solution, V<sub>1</sub> means dilution volume of extracted supernatant, V<sub>0</sub> means initial volume of PBS solution, and W means the weight of starch nanoparticles dissolved in PBS solution.

### Drug release analysis

About 50 mg of drug-loaded starch nanoparticles that possess the most drug loading (2.6 mg/g) under the experimental conditions above was weighed and added to the dialysis tube. Then, 10 mL of PBS solution was added to the dialysis tube. Subsequently, the drug-loaded starch nanoparticles and dialysis tube were placed in a beaker containing 80 mL of PBS solution and slowly stirred in magnetic stirring apparatus at 37°C. At appropriate time intervals, 5 mL of solution was taken out and replaced by the same volume of fresh PBS solution. The cumulative release rate was determined according to the standard curve of indomethacin absorbance to concentration and eqn. (4).

$$Q = \frac{\sum_{i=1}^n C_i V_i + C_n V}{W \times P} \quad (4)$$

where C<sub>i</sub> and C<sub>n</sub> is the mass of indomethacin released from drug-loaded starch nanoparticles at a given time, V<sub>i</sub> is the solution volume got taken out at each time, V<sub>i</sub>=5 ml. V is the cumulative solution volume got taken out, P is the total drug loading in starch nanoparticles. W is the mass of starch nanoparticles, W=50 mg.

### Statistical analysis

All of the sample analyses were conducted in triplicate and the values were expressed as means ± standard error of the mean, statistical analysis were done using SPSS 18.0. Duncan's multiple range tests were used to estimate significant differences among means at a probability level of 0.05 [29-31].

## Results and Discussion

### Structural characterization of [C<sub>3</sub>OHmim]Ac

The <sup>1</sup>H-NMR spectrum was employed to confirm the structure of [C<sub>3</sub>OHmim]Ac, as shown in Figure 1. <sup>1</sup>H NMR (600 MHz, DMSO, 25°C): δ= 9.83 (s, 1H), 7.81 (d, 1H), 7.71 (d, 1H), 4.26 (t, 2H), 3.86 (s, 3H), 3.37 (s, 1H), 2.50 (m, 2H), 1.88 (m, 2H), 1.59 (s, 3H). The ESI-MS technique was used to obtain the molecular weight of the objective product [C<sub>3</sub>OHmim]Ac, and the result of the spectrum is shown in Figure 2. [C<sub>3</sub>OHmim]<sup>+</sup> was detected under the positive ion mode and the mass-to-charge ratio (m/z) was 141.1, which was consistent with the theoretical calculation result (141) of the molecule ion weight for [C<sub>3</sub>OHmim]<sup>+</sup>. The results of <sup>1</sup>H NMR and ESI-MS indicated that the [C<sub>3</sub>OHmim]Ac was synthesized in two steps successfully.

### Phase behaviour

The phase behaviour is essential to study micro-emulsion. Figure 2 shows the phase diagram of [C<sub>3</sub>OHmim]Ac/TX-100+1-butanol/cyclohexane micro-emulsions system at 25°C. A phase boundary line could be seen to separate two-phase region and a single-phase region. It was evident that a stable, clear and transparent single-phase micro-emulsion region could be observed in the range of [C<sub>3</sub>OHmim]Ac or cyclohexane content from 0% to 100% (wt) and it was suitable to study the microstructure of the micro-emulsions.

Apparently, a large single region that extends from [Omim]Ac starch corner to the cyclohexane corner was observed. The blank region was the one-phase micro-emulsion, and the shadow region marked “two phase” was a cloudy region. And a continuous stable single-phase micro-emulsion region could always be observed in the range of the [Omim]Ac-starch or cyclohexane content from 0% to 100% wt [32].

### Conductivity measurement

It is well known that the applications of micro-emulsion depend on its structure. Therefore, it is essential to investigate the structure of micro-emulsion. Conductivity is frequently used to investigate structure and structural changes in micro-emulsions [16,25]. In the [C<sub>3</sub>OHmim]Ac/TX-100+1-butanol/cyclohexane micro-emulsion, one-

phase region can be divided into [C<sub>3</sub>OHmim]Ac/cyclohexane region (marked IL/O), bicontinuous region (marked B) and cyclohexane/[C<sub>3</sub>OHmim]Ac region (marked O/IL), corresponding to the sharp rise, flat and the drop of last in conductivity curve, respectively [26]. As shown in Figure 3, the initial conductivity increased with the increase of the weigh fraction of cyclohexane because of the continuous increase of conductive micro-emulsion droplets, indicating the formation of O/IL micro-emulsions. When reaching a maximum, the nonlinear conductivity decrease revealed that the medium underwent a structural transition and became bicontinuous owing to progressive growth and interconnection of the O/IL microdomains. The further increase of cyclohexane resulted in a linear decrease of conductivity, which was interpreted as the consequence of the formation of IL/O micro-emulsions, suggesting inverse droplet aggregation appeared (Figures 4 and 5).

### FTIR of starch nanoparticles

Figure 4a illustrates the FTIR spectra of native maize starch, OSA modified maize starch and starch nanoparticles. Compared with native maize starch, OSA modified maize starch showed two new absorption bands at 1570 and 1722 cm<sup>-1</sup>. The band occurring at 1570 cm<sup>-1</sup> originated from asymmetric stretching vibration of carboxylate RCOO<sup>-</sup>. The peak at 1722 cm<sup>-1</sup> corresponded to C=O stretching vibration of an ester group [30]. These bands certified the formation of esterification. 1158, 1081, 1015 cm<sup>-1</sup> were assigned to the C-O bond stretching vibrations of anhydroglucose units, meanwhile, the O-H stretching and C-H stretching showed a strong signal at 3354 and 2931 cm<sup>-1</sup>, which is the same as native maize starch [32,33]. The spectra of starch nanoparticles exhibited some difference compared with OSA modified maize starch. The band of which at 3354 and 2931 cm<sup>-1</sup> became narrow and moved to high frequency region. The reason might be that the crosslinking bonds replaced the O-H in starch. The peak at 1015, 1081 and 1158 cm<sup>-1</sup> became stronger compared with OSA modified maize starch because of the formation of interior bonds in cross-link reaction. These data suggested the crosslinking reaction occurred between the starch molecules, and there are similar reports about FTIR spectrogram of starch microspheres.

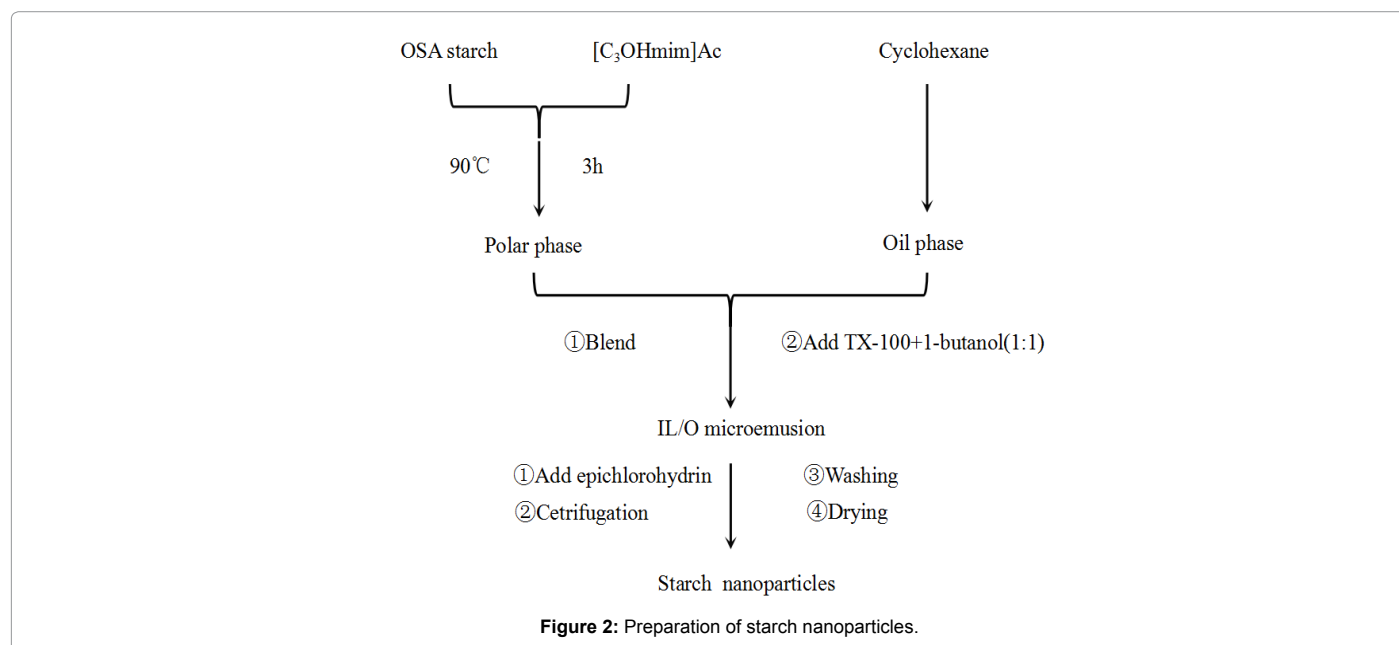


Figure 2: Preparation of starch nanoparticles.

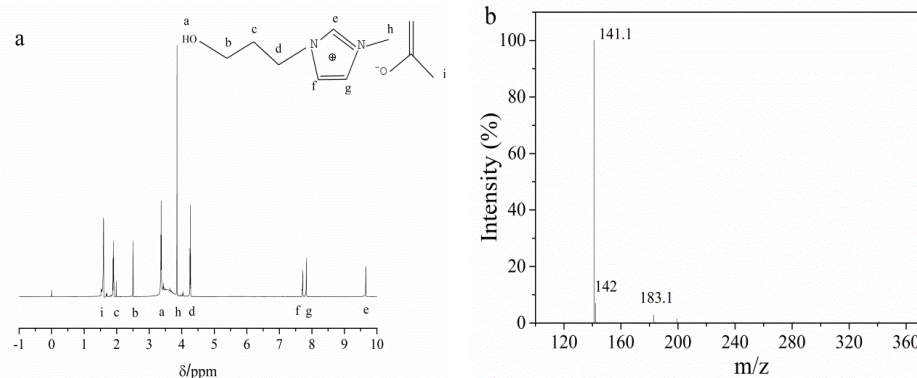


Figure 3: (a)  $^1\text{H}$  NMR spectrum of  $[\text{C}_3\text{OHmim}]\text{Ac}$ . (b) The ESI-MS spectrum of  $[\text{C}_3\text{OHmim}]\text{Ac}$  at positive ion mode.

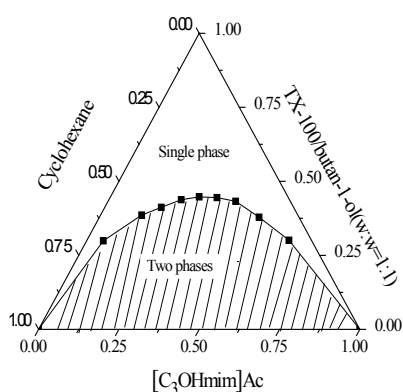


Figure 4: Phase diagram of  $[\text{C}_3\text{OHmim}]\text{Ac}/\text{TX-100}+1\text{-butanol}/\text{cyclohexane}$  at  $25^\circ\text{C}$ .

X-ray diffraction (XRD) was used to study the crystalline structure of native maize starch, OSA modified maize starch and starch nanoparticles, as shown in Figure 4b. We observed that the native maize starch had no difference with OSA modified maize starch in the crystalline structure with the sharp diffraction peaks at  $15.2^\circ$ ,  $16.9^\circ$ ,  $18.1^\circ$  and  $23.2^\circ$ , showing a typical A-type pattern structure. This suggested that OSA modification had little effects on the crystalline structure. On the other hand, the spectrogram of starch nanoparticles showed a big broad peak, indicating that most of crystalline structure of the starch was probably destroyed into the amorphous shape due to the dissolution (Figure 6).

### Morphological analysis of starch nanoparticles

Scanning electron microscopy (SEM) is an effective way to observe the morphology of particles. As seen from Figure 5, native maize starch had the similar morphology compared with OSA modified maize starch, the sizes varied from about 10 to  $20\ \mu\text{m}$  and all of them were polygonal granules. Most of granules showed aggregation or cluster formation which could be mainly attributed to strong van der Waals force and electrostatic attraction, which was in line with Liu et al. [30] who also reported that starch granules congregated together. In comparison with these two starches, starch nanoparticles showed approximately spherical granules with fine dispersibility and were much smaller, their size and distribution of starch nanoparticles were analyzed by DLS technique as shown in Figure 7. The mean diameter of starch nanoparticles was 85.69 nm and the size distribution was relatively concentrated [31].

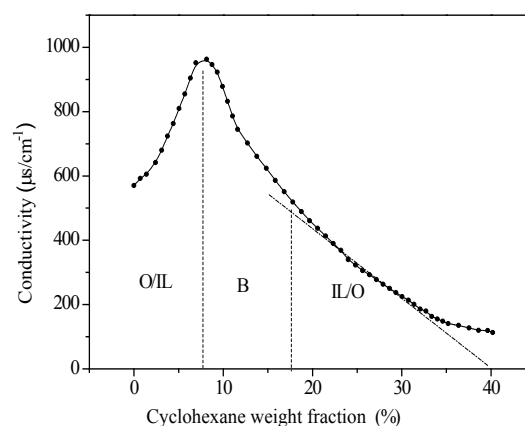
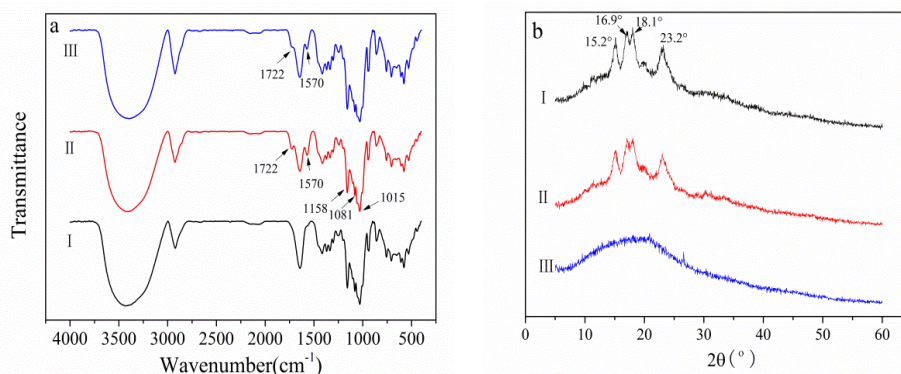


Figure 5: Electrical conductivity as a function of cyclohexane weight fraction in the microemulsion at  $25^\circ\text{C}$ .  $[\text{C}_3\text{OHmim}]\text{Ac}$ : TX-100+1-butanol=1:4 (w/w), TX-100: 1-butanol=1:1(w/w).

### Drug loading analysis

The influence of loading time on drug loading property is shown in Figure 8a. The drug loading and encapsulation efficiency increased first and then decreased as time went on. To be exact, the drug loading increased from 1.12 to 2.63 mg/g as the time was prolonged from 0.5 to 2 h and then decreased to 2.26 mg/g when the time was extended to 2.5 h. The encapsulation efficiency increased from 5.8 to 12.9% and then reduced to 11.8% correspondingly. From the result, it could be concluded that the drug loading and encapsulation efficiency of starch nanoparticles on indomethacin presented an appropriate time value. The effect of temperature on drug loading property is observed in Figure 8b. It was obvious that different loading temperatures resulted in significant changes in drug loading and encapsulation efficiency. At a temperature of  $17^\circ\text{C}$ , starch nanoparticles loaded with more indomethacin and encapsulation efficiency showed the same trend. The reason for this phenomenon may be that the adsorption of indomethacin was mainly attributed to the existence of opposite charges and high affinity. This adsorption process would be hindered by high temperature; thus, the drug loading reduced at higher temperature. Starch nanoparticles with different particle sizes (86, 133, 187 and 263 nm) were obtained through changing the reaction conditions such as reaction time, reaction temperature, and starch concentration to investigate the effect of particle size on drug loading property. As shown in Figure 8c, drug loading and encapsulation efficiency decreased with



**Figure 6:** FTIR spectra (a) and XRD patterns (b) of native maize starch (I), OSA modified maize starch (II) and starch nanoparticles (III)

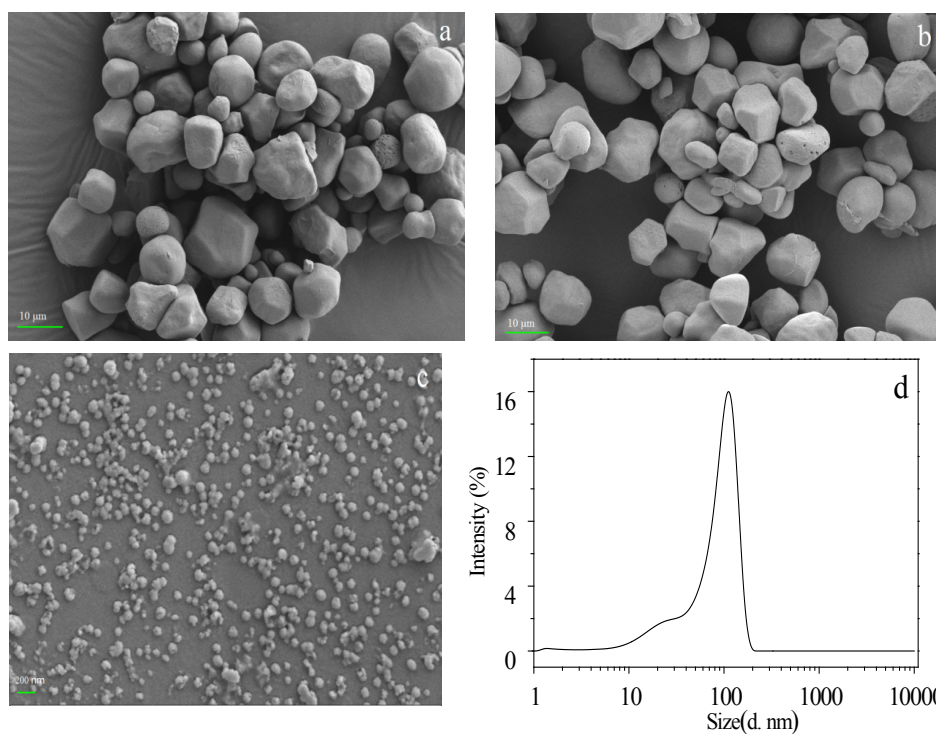


**Figure 7:** SEM images of native maize starch ( $\times 1000$ , a), OSA modified maize starch ( $\times 1000$ , b) and starch nanoparticles ( $\times 20000$ , c) and the particle size and distribution of starch nanoparticles (d).

increasing particle size of starch nanoparticles. The reason for this phenomenon may be that starch nanoparticles of smaller particle size have greater specific surface area and stronger adhesion ability. As shown in Figure 8d, drug loading ascended significantly from 1.35 to 3.75 mg/g as the concentration of indomethacin rose from 0.02 to 0.08 mg/mL. However, the increase of drug concentration caused a decline in encapsulation efficiency. Therefore, higher drug concentration does not necessarily result in better drug loading property.

### Drug release analysis

Drug release experiments were performed in PBS solution. As shown in Figure 9, initially, a burst release was observed in the first 1 h after the starch nanoparticles were immersed into the medium, high release rate of 74.32% was associated with the immediate dispersing of the indomethacin close to starch nanoparticles surfaces. In the following 2 h, the starch nanoparticles formed a swelling-controlled

and sustained release system, in which the release rate slowed down, and 89.75% of the indomethacin contained in the starch nanoparticles was released. This phenomenon was because on the one hand, indomethacin in the nanoparticles which occupied lots free volume spaces inside the swollen nanoparticles created tortuous paths to assist the transportation of water molecules, which facilitated starch nanoparticles to absorb water and swell sufficiently. On the other hand, increasing swelling impeded a great number of indomethacin molecules to diffuse out of the starch nanoparticles and pass into the release medium through numerous pores and channels in the particles. However, as the nanoparticles swelled in PBS solution, a gel diffusion layer took shape gradually which hampered the outward expulsion of indomethacin and brought a sustained slowdown to the indomethacin release. From the 3 to 10 h, drug release experienced a slight but slow rise. 94.52% of the indomethacin was released into PBS solution which kept almost unchanged in the next 10 h. Since the pores

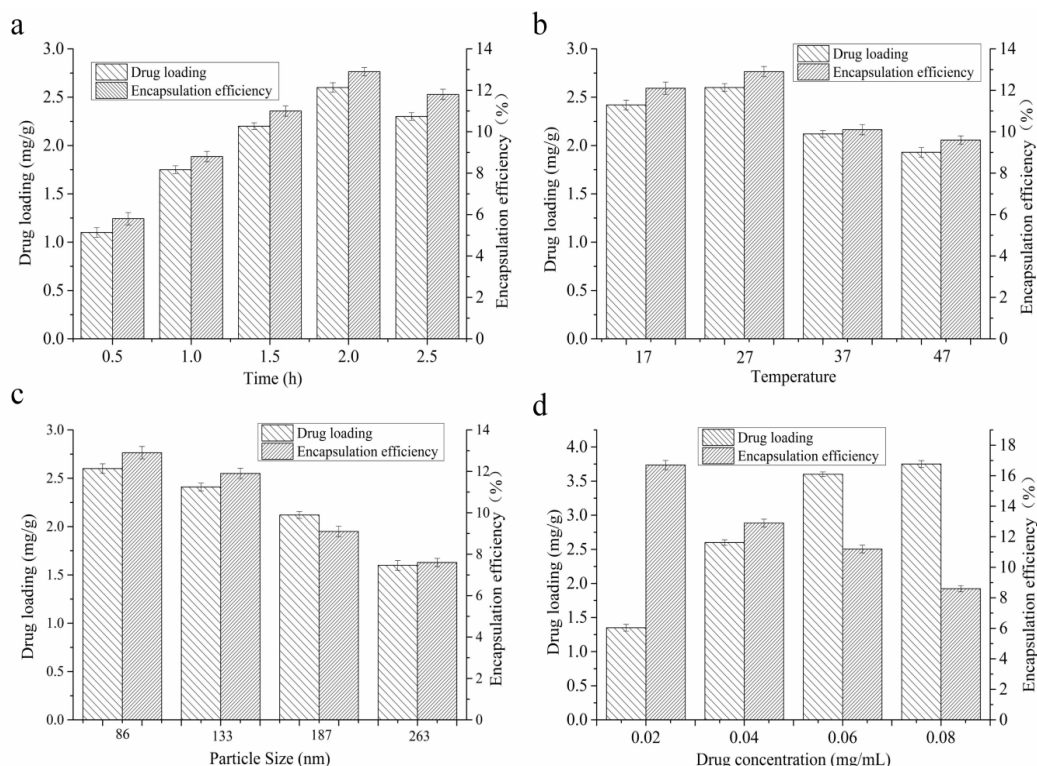


**Figure 8:** Effect of loading time (a), loading temperature (b), particle size (c), and drug concentration (d) on drug loading property. Other conditions: (a) loading temperature, 27°C; particle size, 86 nm; drug concentration, 0.05 mg/mL. (b) Loading time, 2 h; particle size, 86 nm; drug concentration, 0.05 mg/mL. (c) Loading time, 2 h; loading temperature, 27°C; drug concentration, 0.05 mg/mL; (d) loading time, 2h; loading temperature, 27°C; particle size, 86 nm.

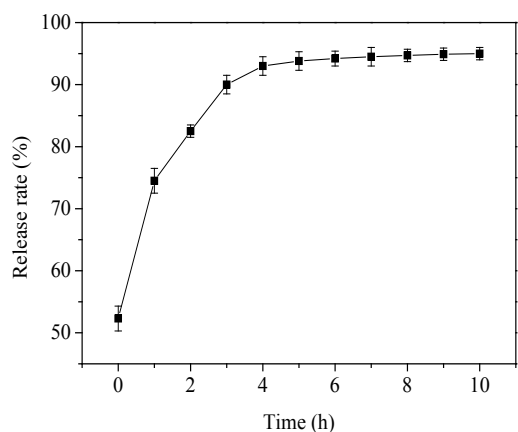


**Figure 9:** Indomethacin release of starch nanoparticles in PBS solution.

and channels for water transportation in the nanoparticles decreased dramatically as the gel diffusion layer enhanced, consequently less and less indomethacin was impelled out of the nanoparticles. Finally, the concentration of indomethacin reached a balance between starch microspheres and PBS solution as time was prolonged. However, tiny amount of indomethacin was released due to gradual but sluggish degradation of starch particles [33].

## Conclusions

In our study, a new room-temperature ionic liquid [C<sub>3</sub>OHmim] Ac, based on imidazolium cation that contained additional functional

group was synthesized to dissolve starch, and molecular structure of [C<sub>3</sub>OHmim]Ac was confirmed by <sup>1</sup>HNMR and ESI-MS. Pseudo-ternary phase diagram conductivity were used to divide the micro region of micro-emulsion. Starch nanoparticles could be prepared based on this micro-emulsion system. FTIR data demonstrated the formation of crosslinking bonds between starch molecules. The spectrum of XRD showed that the crystal structure of starch was destroyed. SEM and DLS intuitively revealed that starch nanoparticles had good sphericity, small size and a relatively concentrated size distribution with the mean diameter was 105 nm.

## Acknowledgements

This research was supported by the National Natural Science Foundation of China (21576098, 21376097), the program for New Century Excellent Talents in University (NCET-13-0212), the Key Project of Science and Technology of Guangdong Province (2016A050502005, 2015A020209015, 2017B090901002), the Key Project of Science and Technology of Guangzhou City (201508020082), Project funded by China Postdoctoral Science Foundation (2016M590787, 2017T100616), and the Fundamental Research Funds for the Central Universities, SCUT (2015ZZ043).

## References

- Miao Z, Li Z, Deng D, Wang L, Liu Y (2010) Novel crosslinked starch microspheres as adsorbents of Cu<sup>2+</sup> Journal of Applied Polymer Science 115: 487-490.
- Hallett JP, Welton T (2002) Room-temperature ionic liquids: solvents for synthesis and catalysis. 2. Ionic liquids in synthesis. Wiley VCH Verlag 111: 3508-3576.
- Dupont J, Souza RFD, Suarez PA (2002) Ionic Liquid (Molten Salt) Phase Organometallic Catalysis Chem Rev 102: 3667-3692.
- Liu W, Budtova T (2013) Dissolution of unmodified waxy starch in ionic liquid and solution rheological properties. Carbohydr Polym 93: 199-206.

5. Mazza M, Catana DA, Vaca-Garcia C, Cecutti C (2009) Supramolecular Polymer Network and Gels 16: 207-215.
6. Fujii K, Soejima Y, Kyoshoin Y, Fukuda S, Kanzaki R, et al. (2008) Electrochemistry in Ionic Liquids. J Phys Chem 112: 4329-4336.
7. Fujii K, Mitsugi T, Takamuku T, Yamaguchi T, Umabayashi Y, et al. (2009) Electrochemistry in Ionic Liquids. Chem Lett 38: 340-341.
8. Jobling S (2004) Improving starch for food and industrial applications. Curr Opin Plant Biol 7: 210-218.
9. Raina C, Singh S, Bawa A, Saxena D (2007) A comparative study of Indian rice starches using different modification model solutions LWT. Food Sci Technol 40: 885-892.
10. Kim M, Lee SJ (2002) Textile Finishing: Recent Developments and Future Trends. Carbohydr Polym 50: 331-337.
11. Mundargi RC, Shelk BN, Rokhade AP, Patil SA, Aminabhavi TM (2008) Formulation and in-vitro evaluation of novel starch-based tableted microspheres for controlled release of ampicillin. Carbohydrate polymers 71: 42-53.
12. Sechia MSN, Marquesa TP (2017) Preparation and Physicochemical, Structural and Morphological Characterization of Phosphorylated Starch.
13. Malafaya P, Stappers F, Reis R (2006) Starch-based microspheres produced by emulsion crosslinking with a potential media dependent responsive behavior to be used as drug delivery carriers. J Mater Sci Mater Med 17: 371-377.
14. Mao S, Chen J, Wei Z, Liu H, Bi D (2004) Intranasal administration of melatonin starch microspheres. Int J Pharm 272: 37-43.
15. Gathergood N, Garcia MT, Scammells PJ (2004) Biodegradable ionic liquids: Part I. Concept, preliminary targets and evaluation. Green Chem 6: 166-175.
16. Gao H, Li J, Han B, Chen W, Zhang J, et al. (2004) Microemulsions with ionic liquid polar domains. Phys Chem 6: 2914-2916.
17. Gao Y, Han S, Han B, Li G, Shen D, et al. (2015) Ionic Liquid-Based Surfactant Science Ionic liquid-Based Surfactant Science. Langmuir 21: 5681-5684.
18. Yan F, Texter J (2006) Surfactant ionic liquid-based microemulsions for polymerization Chem. Commun. (Camb) 25: 2696-2698.
19. Zhang G, Zhou H, Hu J, Liu M, Kuang Y (2009) Ionic Liquid-Based Surfactant Science: Formulation, Characterization and Applications. Green Chem 11: 1428-1432.
20. Zhou G, Luo Z, Fuv X (2014) Preparation of Starch Nanoparticles in a Water-in-Ionic Liquid Microemulsion System and Their Drug Loading and Releasing Properties. J Agric Food Chem 62: 8214-8220.
21. Zhou G, Luo Z, Fu X (2014) Industrial Crops and Products 52: 105-110.
22. Kim MJ, Choi SJ, Lim ST, Kim HK, Heo HJ, et al. (2007) Ferulic acid supplementation prevents trimethyltin-induced cognitive deficits in mice. Bioscience, Biotechnology and Biochemistry 71: 1063-1068.
23. Cheng X, Fu J, Liu J, Zhang Z, Zhang Y, et al. (2007) Ionic Liquid-Based Surfactant Science. Colloid Surface A 302: 211-215.
24. Najjar R, Stubenrauch C (2009) Phase diagrams of microemulsions containing reducing agents and metal salts as bases for the synthesis of metallic nanoparticles. J Colloid Interface Sci 331: 214-220.
25. Wei J, Su B, Liang R, Xing H, Bao Z, et al. (2012) Ionic Liquid-Based Surfactant Science. Colloid Surface A 414: 82-87.
26. Dvornitzky M, Lagues M, Pesant LJ, Ober R, Sauterey C, et al. (1980) A structural description of microemulsions. Small-angle neutron scattering and electrical conductivity study. J Phys Chem 84: 1532-1535.
27. Zheng Y, Eli W, Li G (2009) FTIR study of Tween80/1-butyl-3-methylimidazolium hexafluorophosphate/toluene microemulsions. Colloid Polym Sci 287: 871-876.
28. Pramanik R, Ghatak C, Rao VG, Sarkar S, Sarkar N (2011) Room temperature ionic liquid in confined media: a temperature dependence solvation study in [bmim][BF4]/BHDC/benzene reverse micelles. J Phys Chem 115: 5971-5979.
29. Hong J, Zeng AX, Brennan SC, Brennan M, Han Z (2016) Recent Advances in Techniques for Starch Esters and the Applications: A Review. 5: 50.
30. Liu Z, Li Y, Cui F, Ping L, Song J, et al. (2008) Production of octenyl succinic anhydride-modified waxy corn starch and its characterization. J Agric Food Chem 56: 11499-11506.
31. Kačuráková M, Wilson RH (2001) Renewable Resources for Functional Polymers and Biomaterials. Carbohydr Polym 44: 291-303.
32. Mano JF, Koniarova D, Reis RL (2003) Thermal properties of thermoplastic starch/synthetic polymer blends with potential biomedical applicability. J Mater Sci: Mater Med 14: 127-135.
33. Li ZB, Wang JL, Li D, Adhikari B, Mao HZ (2012) Preparation and characterization of crosslinked starch microspheres using a two-stage water-in-water emulsion method. Carbohydr Polym 88: 912-916.